

Transfer of subcratonic carbon into kimberlites and rare earth carbonatites

PETER J. WYLLIE

Division of Geological and Planetary Sciences, California Institute of Technology, Pasadena, CA 91125, U.S.A.

Abstract—Carbon and volatile components involved in the genesis of kimberlites and carbonatites rise from a mantle reservoir below the asthenosphere. Vapors include the components C–H–O–S–K, in molecular form dependent on the oxygen fugacity, a parameter that varies as a function of depth in ways not yet fully understood. Kimberlites are generated where upward percolating reduced volatile components cross the solidus for peridotite–C–H–O. The depleted, refractory base of the lithosphere, 200–150 km deep, is a collecting site for kimberlite magma at temperatures above its solidus; this layer has been intermittently invaded by small bodies of carbonated kimberlite, through billions of years; most of these aborted and gave off vapors enriching the lower lithosphere by metasomatism, but some reached the surface, through vapor-enhanced crack propagation. Nephelinites and associated carbonatites require upward movement of solid mantle as a plume. Thinning of the lithosphere above a mantle plume, beneath a rift, results in magma trapped in the asthenosphere–lithosphere boundary layer rising with the isotherms, without crossing the solidus until the magma reaches the depth interval 90–65 km, where the solidus for peridotite–CO₂–H₂O becomes subhorizontal, with low dP/dT , pressure independent, and forming a ledge or phase equilibrium barrier. At this level, magma chambers form, and crystallization is accompanied by evolution of vapors, enhancing crack propagation and the eruption of nephelinitic magmas that differentiate to carbonatites. The release of vapors at this level generates another metasomatic layer, at depths known to contain metasomatic RE–titanates. These metasomes may be the source of the REE in carbonatites. Liquidus studies in the system CaCO₃–Ca(OH)₂–La(OH)₃ at 1 kbar demonstrate that residual carbonatite magmas may contain more than 20 weight percent La(OH)₃, as long as the REE were not removed at earlier stages of differentiation by other minerals.

INTRODUCTION

CARBON IS A TRACE element in most igneous rocks, but it becomes a major component in carbonatites, and it plays a significant role in kimberlites. Possible sources of carbon in igneous rocks include shallow-level material of the biosphere, sedimentary or metamorphic limestones, subducted limestones or carbonated ocean–floor basalt, or primordial carbon from the deep mantle.

A general scheme illustrating the inter-relationships of various types of igneous activity in different tectonic environments is presented in Figure 1. The parts of the scheme relevant for this paper are outlined here, and discussed in more detail in following pages. Oceanic basalts contain small concentrations of H₂O and CO₂ certainly derived from the mantle. The submarine basalts react with sea water, with the formation of calcite and hydrated minerals. The oceanic crust when subducted may carry with it in addition pelagic sediments, including slabs of limestone (during the relatively brief period of geological history that pelagic limestones have been formed). During metamorphism and melting of the subducted oceanic crust, it appears that most of the water escapes from the crust to participate in convergent boundary processes. Some of the carbonate may escape these processes and be carried deeper into the mantle for long-term storage of carbon.

Kimberlites intrusions rise from deep within the mantle, near the lithosphere–asthenosphere boundary layer. The diamonds that they transport to the surface have been resident in this region through thousands of millions of years, providing irrefutable evidence that carbon does exist in the mantle. Although diamonds occur only as trace minerals in kimberlites, there is now little doubt that some of the other carbon in kimberlites, consolidated in the form of carbonate, is derived from at least this depth. Carbonatites are formed by differentiation of nephelinitic magmas, commonly in rifted cratonic environments. Limestone assimilation has been invoked in the petrogenesis of alkaline magmas, but most investigators now agree that the carbon in carbonatites was derived from the deep source of the alkalic magmas. Mantle carbon may be primordial, or derived from subducted oceanic crust.

The geochemistry of the magmas represented in Figure 1 is currently interpreted in terms of melts derived from distinct mantle and crustal source reservoirs, contaminated to greater or lesser extent by metasomatic fluids. Some magmas have trace element and isotope fingerprints indicating that they have components derived from more than one source. The geochemistry of carbon with respect to the location and evolution of these reservoirs is an important problem still poorly understood.

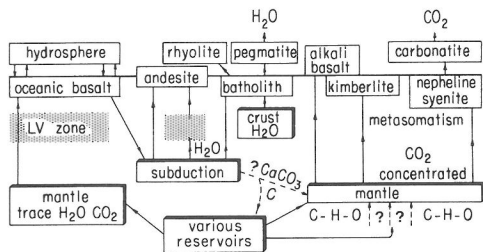


FIG. 1. Generalized cycle illustrating the distribution of H_2O and CO_2 among igneous rocks and their crust and mantle sources. From left to right, the tectonic environments represented are: divergent oceanic plate boundary, convergent plate boundary, and continental platform, with rifting.

SUBDUCTION OF OCEANIC CRUST

The main attention to subducted igneous crust in the context of igneous petrology has been in connection with the origin of calc-alkaline igneous rock series. Water is generally considered to be the dominant volatile component, although the large masses of carbon dioxide given off from andesitic cones have been attributed to sources in the subducted crust. The phase relationships required to trace the fate of calcite or dolomite in subducted oceanic crust have been determined (HUANG *et al.*, 1980; HUANG and WYLLIE, 1984, Figure 7). As a first step in study of melting relationships between eclogite and carbonate, OTTO (1984) and OTTO and WYLLIE (1983) determined the melting relationships of calcite in contact with albite-jadeite at 25 kbar. The near-solidus liquid contains more than 50% dissolved $CaCO_3$. HUANG *et al.* (1980) concluded that there is a prospect that some carbonates in subducted oceanic crust would escape dissociation and melting, be converted to aragonite, and be carried to considerable depths for long-term storage in the mantle. Calcite should react with adjacent peridotite to yield dolomite or magnesite (WYLLIE *et al.*, 1983), but according to current views on the redox state of the upper mantle, carbonate carried into the mantle should eventually become reduced to graphite or diamond (RYABCHIKOV *et al.*, 1981; HAGGERTY, 1986).

THE GENERATION AND ERUPTION OF KIMBERLITES

In order to locate the positions within the upper mantle for the generation of kimberlite magmas, we need to know the compositions of the rocks at various depths, their phase relationships as a function of depth and volatile contents, with particular attention to the solidus curves and the compositions

of near-solidus liquids, and the position of the geotherm. A compilation of some of these data is given in Figure 2. In order to decipher the process of eruption of kimberlites, we need to know the thermal history of the region at depth, which is a consequence of physical processes and the physics of the solid-melt-vapor systems.

Geotherms beneath cratons

From the geothermometry and geobarometry of peridotite nodules transported to the surface by kimberlites and alkali basalts, the geotherm for cratons is consistent with geotherms calculated from heat loss. The fossil geotherm for many kimberlites

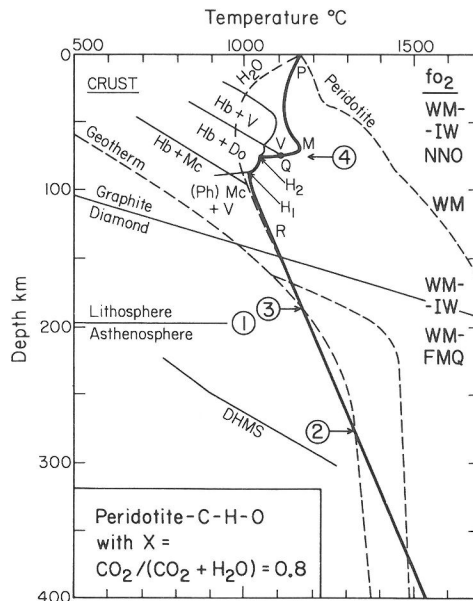


FIG. 2. Solidus curves for peridotite- H_2O and for peridotite- CO_2 - H_2O with defined ratio of CO_2/H_2O (see Figure 10), compared with cratonic geotherm, with and without inflection (BOYD and GURNEY, 1986). For phase equilibrium background and sources, see WYLLIE (1977, 1978, 1979) and EGGLE (1978b). The positions of selected phase boundaries relevant to mantle processes and the origin of kimberlites and nephelinites are given, and discussed in the text. Level (1) corresponds to the depth of the lithosphere-asthenosphere boundary, points (2) and (3) are depth levels limiting the interval within which magma can be generated (in the presence of fluids) for the particular geotherm, and level (4) corresponds to the change in slope of the solidus curve near point Q. The oxygen fugacities at various levels are indicated by the buffers listed (HAGGERTY, 1987). Peridotite solidus from TAKAHASHI and SCARFE (1985). For DHMS (dense hydrated magnesian silicates) see RINGWOOD (1975, p. 295). Abbreviations: Hb = amphibole, Ph = phlogopite, Do = dolomite, Mc = magnesite, V = vapor. See also Figures 7 and 8 for discussion of R, H₁, H₂, V, Q, M and P.

(corresponding to the time of eruption) is inflected to higher temperatures at a depth of about 175 km, somewhat deeper than the graphite to diamond transition. Two geotherms are depicted in Figure 2, one with and one without an inflection (BOYD and GURNEY, 1986). The inflection has been interpreted in terms of uprise of mantle diapirs associated with the generation of kimberlites, or in terms of local magma chambers, or as due to materials having different thermal conductivities.

Phase relationships

The phase relationships for the system peridotite-CO₂-H₂O, involving the minerals amphibole, phlogopite, dolomite and magnesite (see Figure 2 for an example), provide the framework for upper mantle petrology. There is abundant evidence in fluid inclusions for the passage of H₂O and CO₂ through the lithosphere (*e.g.*, ANDERSEN *et al.*, 1984). The redox state of the deeper mantle, however, appears to be such that the components C-H-O exist as carbon and H₂O with CH₄, rather than as CO₂ and H₂O (DEINES, 1980; RYABCHIKOV *et al.*, 1981). HAGGERTY (1986) considered fluids in the asthenosphere to be relatively oxidized (between FMQ and WM buffers), within the field for CO₂ (and therefore, presumably, of carbonate), and concluded that these fluids would be reduced to microdiamonds when released into the more reduced lithosphere, between the WM and IW buffers. HAGGERTY (1987) concluded that a layer of the lithosphere between 60 and 100 km depth has been metasomatized and oxidized up to the NNO buffer. Figure 2 summarizes the possible variations of oxygen fugacity in terms of standard buffers down to 250 km. The phase relationships in the reduced system peridotite-C-H-O have been analyzed in detail by WOERMANN and ROSENHAUER (1985) (see also GREEN *et al.*, 1987). MEYER (1985) reviewed the distribution and redox state of C-H-O in the mantle in connection with the origin of diamonds. HOLLOWAY and JAKOBSSON (1986) presented data on the distribution of C-H-O components between liquid and vapors, with applications to oxygen fugacities in mantle and volcanic gases.

With low oxygen fugacities at high pressures, fluids in the system C-H-O exist as H₂O with CH₄ or graphite/diamond. Under these conditions, it appears that the peridotite-C-H-O solidus may remain close to that for peridotite-H₂O, with carbonate ions being generated in the melt when CH₄ or graphite/diamond dissolves (EGGLER and BAKER, 1982; RYABCHIKOV *et al.*, 1981; WOERMANN and ROSENHAUER, 1985). In the following

discussion, therefore, the extrapolated solidus for peridotite-H₂O, which I believe to be very close to that for peridotite-CO₂-H₂O at pressures greater than about 35 kbar (WYLLIE, 1978; ELLIS and WYLLIE, 1980), is adopted as the solidus at depth for peridotite-C-H-O. The extrapolated solidus curves given in Figure 2 correspond closely to those adopted previously in consideration of the origin of kimberlite (WYLLIE, 1980), and the qualifications stated then will not be repeated. The solidus for mixed volatile components is for CO₂/(CO₂ + H₂O) = 0.8. With variation in this ratio the solidus temperature changes at pressures shallower than point Q at about 75 km, but remains unchanged at higher pressures (see WYLLIE, 1978, 1979; EGGLER, 1978b, for details). More detailed evaluation of the phase relationships at pressures between 50 and 100 km depth will be presented below, in connection with the origin of nephelinites and carbonatites.

Critical depth levels

There are four levels in the upper mantle, identified in Figure 2, where critical changes occur in the physical processes that control the composition and mode of migration of the low-SiO₂, volatile-rich magmas erupted in cratonic environments. The first critical level, (1), is the depth of the lithosphere-asthenosphere boundary layer, through which the mantle flow regime changes from convective (ductile) to static (brittle). A depth of 200 km is commonly adopted for this level in subcratonic mantle, corresponding approximately to the 1200°C isotherm. The two depths where the solidus is intersected by the local geotherm, (2) and (3), limit the depth interval within which magmas can be generated. The fourth level, (4), is the narrow depth interval near Q in Figure 2 where the solidus changes slope, and becomes sub-horizontal, with low dP/dT . The depth of level (4) differs according to different investigators (see review below). Levels (2), (3) and (4) are different for lherzolites and harzburgites (WYLLIE *et al.*, 1983); compared with lherzolite the solidus for harzburgite is higher, and therefore the levels (2) and (3) are deeper, and level (4) is also deeper. The depths of levels (1), (2) and (3) vary from place to place and from time to time, as a function of the geotherm and local history.

Other important levels in the mantle are those where volatile components would be released by activation of a dissociation reaction. One such reaction is represented in Figure 2 by the line DHMS giving the boundary for the reaction of olivine to form dense hydrous magnesian silicates in the presence of H₂O. The estimated position of the reaction

for the conversion of forsterite to brucite and enstatite in $\text{MgO-SiO}_2\text{-H}_2\text{O}$ is close to the DHMS curve at 300 km (ELLIS and WYLLIE, 1979, 1980).

Processes

An interpretation of the processes involved in the origin of kimberlites is given in Figure 3 (WYLLIE, 1980). The solidus corresponds to that in Figure 2, with somewhat higher estimated temperature for M. Reduced volatile components rising up the geotherm cross point *a* (level 2), with the formation of a trace of interstitial melt. Increased concentration of melt results in density instability, followed by uprise of diapirs. In this current modification of the 1980 treatment, motion of the diapirs is slowed or stopped as they enter the base of the lithosphere at level (1). If the melt cools sufficiently to release vapor, a crack may propagate from level *c*, releasing kimberlite magma for intrusion into the crust or eruption. Under these circumstances, the magma passes right through level (4) without being affected by the peridotite phase relationships. A more common fate for such small magmatic excursions, according to SPERA (1984), is solidification at depth through thermal death.

If the melts are not stopped by the rheological change at level (1), the asthenosphere-lithosphere boundary, they may continue to rise along adiabats, as represented by path *a-f* in Figure 4 (in which case, only minor melting occurs), or they may follow a path only slightly elevated above the geotherm, represented by *a-e* (SPERA, 1984). As the magmas approach the solidus from below, remaining in equilibrium with host lherzolite, crystallization

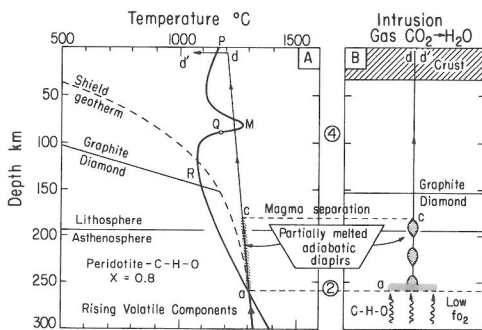


FIG. 3. Solidus and geotherm controls on the generation of magma in mantle peridotite with a flux of volatile components inducing adiabatic uprise of partially melted diapirs. The diapirs fail to penetrate far into the lithosphere. Under suitable tectonic conditions, with release of vapor enhancing crack propagation, kimberlite magma is intruded into the crust from depth *c* (modified after WYLLIE, 1980).

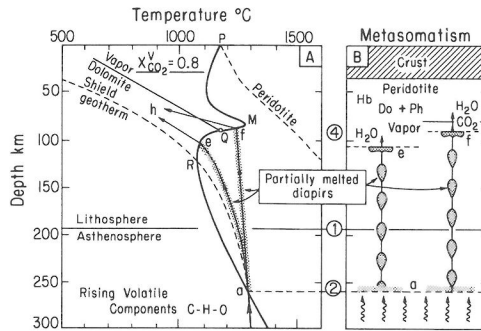


FIG. 4. Solidus controls on the upward migration of partly melted diapirs through lithosphere, following adiabatic or shallower paths of uprise. Compare Figure 3. Crystallization and evolution of vapors occurs at the solidus, M-Q-R, and the mantle above can become strongly metasomatized (modified after WYLLIE, 1980).

proceeds at *f* or *e* and vapor is evolved. The overlying mantle is subjected to extensive metasomatism. HAGGERTY (1987) concluded independently from study of mantle nodules that there is a metasomatized horizon between 100 km and 60 km depth. Magma chambers may develop at positions *e* and *f*. The point Q is significant because at shallower levels the composition of vapor released is the same as the ratio of $\text{CO}_2/\text{H}_2\text{O}$ in the system, whereas at greater depths the vapor is progressively enriched in H_2O (WYLLIE, 1978, 1979, 1980). The compositions of melt and vapors associated with the solidus in the region of level (4), MQR in Figure 4A, vary widely for quite small changes in conditions. Many alkalic magmas are probably derived from parental magmas generated in this region. Note that adiabatic paths for diapirs of higher temperature, rising from greater depths, would miss the solidus at M; these might reach the solidus for peridotite, with generation of basaltic magmas. Similarly, if the ratio $\text{CO}_2/\text{H}_2\text{O}$ was lower, the temperature of point M would be lower and again, the diapirs could rise past this level without encountering the solidus.

Consider the craton in Figure 5 with normal, undisturbed geotherm, composed largely of lherzolite with a concentration of harzburgite in its lower part, between about 170 and 200 km depth, along with pods of eclogite (SOBOLEV, 1977; BOYD and GURNEY, 1986; HAGGERTY, 1986). No magma is generated unless volatile components are present or are introduced into the depth level between 270 km and 185 km (levels 2 and 3 in Figure 2). For the geotherm and solidus given in Figures 2, no vapors or carbonate can exist between (2), 275 km, and (3), 180 km, because they would be dissolved in

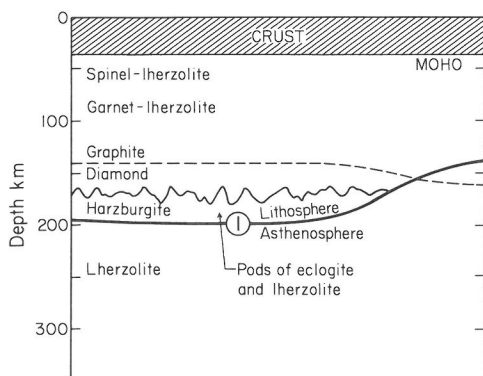


FIG. 5. Simple petrological cross-section of a craton, with depleted keel of harzburgite containing macrodiamonds (SOBOLEV, 1977; BOYD and GURNEY, 1982, 1986).

melt (WYLLIE, 1980, Figure 4). Therefore, the generation of new melt is dependent on the uprise of volatile components from depths greater than (2). Note that the reactions of olivine with water to form DHMS or brucite probably intersect the geotherm somewhere between 300–400 km, suggesting that perhaps only highly reduced gas, CO, CH₄ and H₂, can exist at deeper levels.

Assume that a part of the lithosphere is in the early stages of rifting, initiated by an increase in heat flow supplied by a mantle plume from the deep mantle. Sparse volatile components entrained in the rising plume, enhanced by release of H₂O from DHMS and brucite (WOERMANN and ROSENHAUER, 1985), if present, will generate interstitial melt at level (2), where the lherzolite is transported across the solidus curve (compare Figures 3 and 4). Figure 6 illustrates the plume diverging laterally below level (1), the asthenosphere–lithosphere boundary. As it diverges, the melt becomes concentrated in layers or chambers in the boundary layer above the plume. This aggregation is associated with local uprise of the geotherms, and thinning of the lithosphere. Lateral divergence of the asthenosphere transports some of the entrained plume melt, which later penetrates the lithosphere, forming small dikes or magma chambers.

The magmas entering the depleted lithosphere, both above the plume and laterally beneath the undisturbed craton, remain sealed within the more rigid lithosphere, maintained at temperatures above the solidus for lherzolite–C–H–O. The magmas have no tendency to crystallize nor to evolve vapors unless they reach level (3), 10–15 km above the asthenosphere–lithosphere boundary. Contact of the lherzolite–derived magma with harzburgite, however, should result in reaction and the precipi-

itation of minerals through magma contamination. This slow process could lead to the more or less isothermal growth of large minerals resembling the discrete nodules in kimberlites.

Those magmas managing to insinuate their way near to level (3), the solidus, will evolve H₂O–rich vapors. CO₂–rich vapors cannot exist in this part of the mantle (WYLLIE, 1978, 1979; EGGLE, 1978b). They will either be reduced by thermal cracking (HAGGERTY, 1986) yielding microdiamonds that join the old macrodiamonds resident in the depleted keel of the craton through thousands of millions of years, or cause partial melting in lithosphere lherzolite, or they will react with harzburgite to produce magnesite and consequent enrichment of the vapor in H₂O. The vapors may also promote crack propagation, resulting in rapid uprise of the kimberlite magma. Many intrusions from this level will solidify before rising far (SPERA, 1984), but others will enter the crust as kimberlite intrusions (ARTYUSHKOV and SOBOLEV, 1984). Kimberlites may be erupted either from the early magma accumulating above the plume, or from the lateral magma chambers in the lithosphere base. Magnesite–harzburgite nodules would be disrupted by explosive dissociation of the carbonate during uprise,

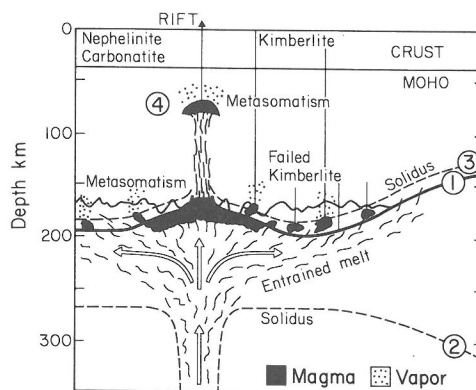


FIG. 6. Magmatic consequences of a deep mantle plume carrying volatile components across the solidus at level (2), with concentration of magma chambers above the plume at the asthenosphere–lithosphere boundary, and entrainment of melt in flowing lherzolite of the asthenosphere. The latter melt enters the boundary layer of the lithosphere in small dikes or magma chambers. If the magma approaches the solidus, level (3), evolution of vapor enhances crack propagation, permitting some kimberlite magmas to reach the crust (see Figure 3). Thinning of the lithosphere above the plume results in upward migration of the magma to level (4), where magma chambers develop, and vapor is evolved with strong metasomatic effects (compare Figure 4). This level is the source of parent magmas for nephelinitic volcanism, and the associated carbonatites.

which provides a satisfactory explanation for the correlation between low-calcium garnets and diamonds in the kimberlites of the Kaapvaal craton (BOYD and GURNEY, 1982; WYLLIE *et al.*, 1983), and in USSR (SOBOLEV, 1977).

THE SOURCE OF NEPHELINITIC VOLCANISM AND CARBONATITES

Alkalic magmatism is commonly associated with doming and rifting on cratons. There is evidence that beneath major rifts the lithosphere is thinned (GLIKO *et al.*, 1985). In Figure 6, the continued heat flux from the rising plume, and the concentration of hotter magma at the asthenosphere–lithosphere boundary, will promote further thinning of the lithosphere. According to GLIKO *et al.* (1985), it takes only several million years for lithosphere thickness to be halved when additional heat flow of reasonable magnitude is applied to the base of the lithosphere. The igneous sequence associated with this process was discussed by WENDLANDT and MORGAN (1982). The magma near the boundary layer at levels (1)–(3) will rise with the boundary layer, either percolating through the newly deformable matrix, or as a series of diapirs, with the amount of liquid increasing in amount as the boundary layer rises, extending further above the solidus for peridotite–C–H–O. This magma intersects the shallower solidus for peridotite–CO₂–H₂O at level (4) (compare Figures 2, 3, and 4), in the depth range 90–70 km. Magma chambers may be formed as the magma solidifies, and vapors will be evolved causing metasomatism in the overlying mantle, and causing intermittent crack propagation, which releases magmas through the lithosphere. The metasomatic vapors will be aqueous if released at depths greater than Q (Figures 2 and 4), and CO₂-rich if released at depths shallower than Q (HAGGERTY, 1987). A variety of alkalic magmas may be generated at level (4), depending sensitively upon conditions. Magmas rising from this level may include the parents of olivine nephelinites, melilite-bearing lavas, and other igneous associations differentiating at shallower depths to carbonatites.

Phase relationships

There are large changes in the compositions of melts and vapors in the region of level (4) for small changes in pressure and temperature (WYLLIE, 1978; WENDLANDT and EGGLER, 1980; WENDLANDT, 1984). Detailed knowledge of the phase relationships in this region are, therefore, essential for understanding the petrogenesis of alkaline rocks. In previous interpretations of the geometrical ar-

rangements of divariant surfaces in this region, based on available experimental data, it appeared that the amphibole surface would not overlap the dolomite–peridotite–vapor solidus curve, M–Q–R in Figures 3 and 4 (WYLLIE, 1978, 1979). The geometrical relationships for the system were illustrated as a guide for rock systems in which these two-phase elements might overlap. The relationships are shown in Figures 7A and B from WYLLIE (1978). Figure 7C represents the phase relationships for a rock with less H₂O (0.4 weight percent) and CO₂ (5 weight percent) than that required to make the maximum amount of amphibole and dolomite, respectively, in the peridotite. The vapor–absent field for amphibole–dolomite–peridotite extends across the solidus curve defined by the amphibole buffer, m₂–H₂, and the dolomite buffer, H₁–N (part of QR in Figures 3 and 4). For a rock with a higher ratio of CO₂/H₂O, a small field for peridotite + vapor would appear in the region of m₂–H₂ where the amphibole field does not reach the solidus (see Figure 7 in WYLLIE, 1979, and Figures 10C and D). EGGLER (1978a) constructed the dolomite peridotite–vapor solidus curve I₆–N (Figure 7B) with a pressure minimum, which carried it across the amphibole stability surface at a lower pressure than depicted in Figure 7.

Two experimental studies on amphibole–dolomite–peridotite indicate that the amphibole stability volume does overlap the solidus with dolomite, with results shown in Figures 8A and B. The points H₁ and H₂ correspond to the same points in Figure 7. There is a difference of several kbar between the results of BREY *et al.* (1983) in Figure 8A and those from the detailed investigation of OLAFSSON and EGGLER (1983) in Figure 8B. I have interpreted these two sets of experimental results in terms of the topology given in Figure 7 (WYLLIE, 1987), and conclude that the simplest interpretation indicates that there is a discrepancy related to the position of the invariant point I₆ in Figure 8C for the system peridotite–CO₂. The point E76 is EGGLER's (1978b) determination of the point in the model system CaO–MgO–SiO₂–CO₂, where the low-pressure solidus curve for peridotite–CO₂ is succeeded by the high-pressure solidus curve for dolomite–peridotite–CO₂. It is this fundamental change that is responsible for the solidus ledge on the peridotite–CO₂–H₂O solidus, described above as level (4) (Figures 2, 3, and 4). According to the present interpretation of the results in Figure 8A, the point is near 25 kbar (G in Figure 8C), and for the results in Figure 8B it is near 17 kbar (OE in Figure 8C). This difference in pressure amounts to almost 30 km within the mantle.

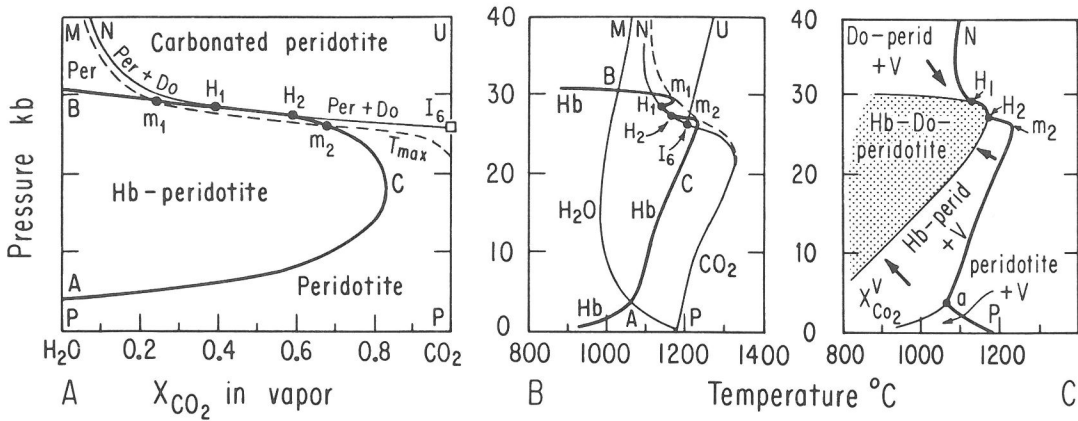


FIG. 7. An example of the topology of the phase relationships for peridotite-CO₂-H₂O if the amphibole stability range overlaps the solidus curve I₆-N (Q-N) for dolomite-peridotite-vapor. Figures 7A and 7B are after WYLLIE (1978). For abbreviations, see Figure 8. A. PX projection of the solidus surface and vapor buffer lines. Between H₁ and H₂ amphibole-dolomite-peridotite begins to melt in the presence of the specified buffered vapor phase composition (mol fraction). B. PT projection showing the amphibole buffer line ACB passing over the temperature maximum on the solidus surface (m₁-m₂), and down to the dolomite buffer line I₆ between H₁ and H₂. C. Isoleth for peridotite with CO₂ and H₂O below amounts required to generate maximum possible dolomite and amphibole, for the condition of overlapping amphibole stability field in Figures 7A and 7B. The solidus is the heavy line: compare with the reported experimental solidus curves in Figures 8A and 8B. The heavy arrows show direction of increasing CO₂/H₂O in subsolidus areas. The shaded area is vapor-absent.

In an effort to resolve this discrepancy, the position of I₆ has been determined using an assemblage of natural minerals corresponding to a lherzolite

(WYLLIE and RUTTER, 1986). The preliminary experimental value at 21 kbar is between the two values deduced from the experiments in Figures 8A

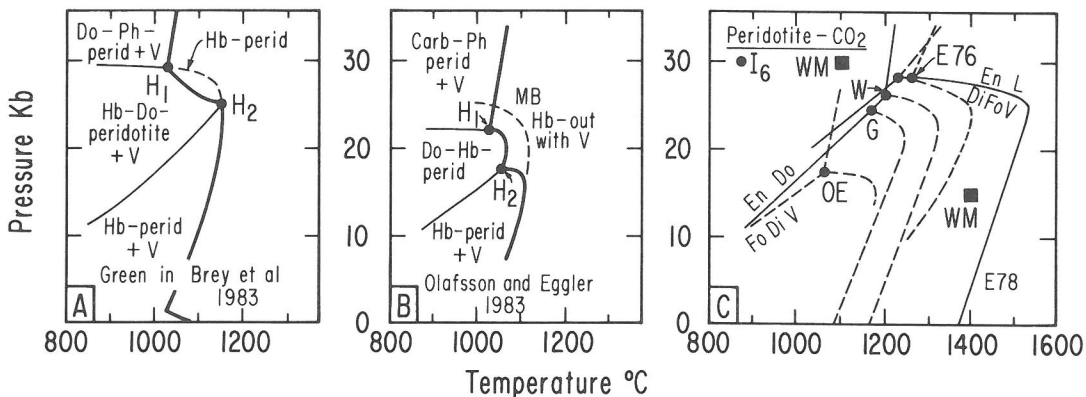


FIG. 8. A and B. Experimentally determined solidus curves for defined compositions in peridotite-H₂O-CO₂, with some interpretation of subsolidus phase fields for comparison with Figure 3. Note the subsolidus assemblage between H₁ and H₂ with vapor, (A), and without vapor, (B). The dashed curve, MB, is the amphibole-out curve in the same rock with H₂O. C. Locations for the invariant point I₆ on the solidus for peridotite-CO₂ deduced or estimated from experimental data in other systems. E78-E76 (solid lines) was experimentally determined in the model system CaO-MgO-SiO₂-CO₂ by EGGLEY (1978b), and he estimated the adjacent dashed curves for peridotite from these results (EGGLEY, 1976). Point W was estimated by WYLLIE (1978). G and OE are deduced from the experimental results given in Figures 8A and 8B, respectively. WM are two experimental points on the solidus for peridotite-CO₂ (WENDLANDT and MYSEN, 1980). Abbreviations: Hb = amphibole, Do = dolomite, carb = carbonate, Ph = phlogopite, Di = diopside, En = enstatite, Fo = forsterite, V = vapor, L = liquid, perid = peridotite. MB = MYSEN and BOETTCHER (1975).

and 8B. This result, in conjunction with those in Figures 8A and 8B, contributes to the reconstruction of the phase relationships in the system amphibole-dolomite-peridotite for a variety of volatile contents and ratios of $\text{CO}_2/\text{H}_2\text{O}$. All previous investigators have assumed that the point I_6 for peridotite is in the range 27–29 kbar, close to that in the synthetic system. Determination of its position at lower pressures results in significant changes in the shapes of the overlapping surfaces for dolomite, amphibole and the solidus, although the topology remains the same. In particular, the highest temperature on the peridotite- CO_2 solidus is reduced, and consequently the temperature of the maximum on the solidus for peridotite- CO_2 - H_2O (M at level 4 in Figures 3 and 4) is also reduced.

Consider first the shapes of the divariant solidus surfaces for peridotite-vapor and for dolomite-peridotite-vapor, without consideration for amphibole. These are depicted by contours on the surfaces for constant vapor-phase compositions (WYLLIE, 1978). Figure 9 shows the solidus curves for peridotite- CO_2 , peridotite- H_2O , and for peridotite in the presence of the successive vapor phase compositions indicated. The line QR is the dolomite-peridotite-vapor buffer line shown in Figures 3 and 4. Note that the extent of the sub-horizontal level (4) is reduced with increasing $\text{H}_2\text{O}/\text{CO}_2$, as Q migrates along the curve I_6 -R. EGGLER's (1978a) interpretation has Q passing through a pressure minimum between I_6 and R.

Figure 10 is a similar diagram showing the intersections of the amphibole stability surface with the divariant surfaces for dolomite formation, and

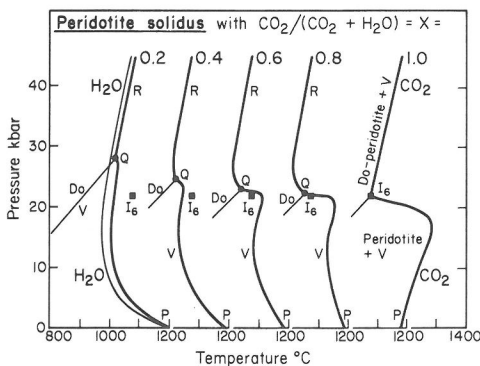


FIG. 9. The system peridotite- CO_2 - H_2O , with excess CO_2 and H_2O . Contours for two parts of the solidus surface, the peridotite-vapor surface from low pressures to the line I_6 -Q-R, and the dolomite-peridotite-vapor surface extending to higher pressures from the line I_6 -Q-R. Contours are plotted in terms of mol fraction of CO_2 in the vapor phase. Revised from WYLLIE (1978).

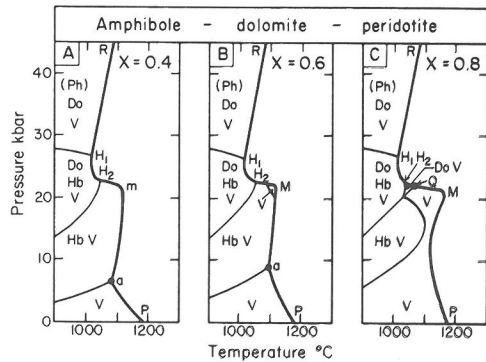


FIG. 10. Buffered solidus curves for amphibole-dolomite-peridotite-vapor with amphibole stability volume crossing the dolomite-peridotite-vapor buffer line I_6 -N (Figure 7), I_6 -R (Figure 9). Revised from WYLLIE (1979, Figures 6B and E, 7) with mol ratios of $\text{CO}_2/(\text{CO}_2 + \text{H}_2\text{O}) = X$. Note the section of solidus H_1 - H_2 with vapor, contrasted with H_1 - H_2 in Figures 7C and 8B without vapor. For abbreviations, see Figure 8.

for the solidus with excess vapor. The amphibole stability field overlaps the solidus surface, generating a buffered solidus curve for amphibole-peridotite-vapor when $\text{CO}_2/\text{H}_2\text{O}$ is somewhat reduced (Figures 10B and 10A). The field for amphibole-dolomite-peridotite is situated between the amphibole and dolomite fields (compare Figures 7 and 8). Figure 10C is the diagram used in Figure 2. Comparison of Figure 10C with the curves PMQR in Figures 3 and 4 indicates that changing the position of I_6 from about 28 kbar to 21 kbar reduces the maximum temperature of the subhorizontal solidus ledge at level (4), and reduces the sharpness of the temperature maximum on the solidus at M (for high $\text{CO}_2/\text{H}_2\text{O}$; compare Figure 9). According to Figure 10, however, there is a substantial ledge on the solidus at this level for every peridotite containing H_2O and CO_2 , regardless of the ratio, which is borne out by the two sets of experimental data in Figures 8A and 8B. If H_2O and CO_2 contents are less than those required to make the maximum amphibole and dolomite, respectively, then the vapor-absent solidus for amphibole-dolomite-peridotite in Figure 10 would form another ledge between H_1 and H_2 (see Figures 7C and 8B).

ORIGIN OF CARBONATITES

As outlined above, the most likely source for the parent magmas of the alkaline complexes with carbonatite intrusions is in the metasomatized upper mantle at depth level (4), associated with the abrupt change in slope of the peridotite- H_2O - CO_2 solidus (Figures 2, 4, and 6). Although the parent melts are

derived from reduced materials at deeper levels (e.g., Figures 4 and 6), they are relatively oxidized by the time they reach the 85–65 km depth level (4) (HAGGERTY, 1987).

Carbonatites are magmatic in origin, commonly derived by differentiation from a parent nephelinitic magma. Fractional crystallization plays a role in differentiation, but liquid immiscibility, *i.e.*, splitting a nephelinitic magma into an ijolite and a carbonatite magma, is another important process. LE BAS (1977) reviewed these topics in detail. The discovery that near-solidus melts in dolomite–peridotite have compositions corresponding to those of carbonatites (WYLLIE and HUANG, 1975; WENDLANDT and MYSEN, 1980) has led to renewed speculation that some carbonatites might be primary, but in most alkaline complexes the volume relations and the time sequence of intrusion appear to favor the derivative origin.

Rare earth carbonatites and phase relationships

Light rare earth elements are concentrated in carbonatites. PECORA (1956) distinguished two varieties of carbonatites, the apatite–magnetite and the rare–earth mineral varieties. Many carbonatites of the apatite–magnetite type, however, do contain REE in monazite. HEINRICH (1966, p. 157) noted that if the term “rare–earth carbonate type” is used, the schism is more pronounced and paragenetically more significant. Bastnaesite is the most abundant RE carbonate in carbonatites, containing up to 64 weight percent REE. There are two problems associated with rare–earth carbonate carbonatites. One is the original source of the rare earth elements, and the other is the process of their concentration.

The source is probably the layer of metasomatized subcontinental lithosphere represented at level (4) in Figures 4 and 6, and characterized in terms of chemistry and mineralogy by HAGGERTY (1987). Haggerty concluded that the existence of upper-mantle metasomes is virtually a prerequisite to the genesis of alkali melts with elevated (silicate–) incompatible element signatures. Among the new minerals discovered in association with spinels in depleted mantle peridotites less than 100 km are titanates enriched in rare earth elements (HAGGERTY *et al.*, 1986; HAGGERTY, 1987). Involvement of these minerals in magmatic processes at level (4) may provide the initially elevated rare earth element concentrations that can lead through differentiation to the formation of rare–earth carbonate carbonatites.

The RE–carbonate type of carbonatite usually represents the last stage in a series of carbonatitic

differentiates, and is normally subordinate to earlier carbonatite. Under some conditions, as in the Mountain Pass carbonatite, with 15 volume percent of the ore body composed of bastnaesite, very high concentrations of RE carbonates are produced.

JONES AND WYLLIE (1983, 1986) have approached the petrogenetic problem in two ways. The first is to build from simple to more complex phase diagrams in order to establish precisely the behavior of rare earth elements in carbonate–rich melts, as a guide for the interpretation of the more complex systems and of the rocks themselves. The second approach is to melt complex mixtures approximating the composition of the ore body at Mountain Pass, to follow paths of crystallization, and to determine the conditions for precipitation of bastnaesite.

The phase relationships in the join CaCO_3 – Ca(OH)_2 – La(OH)_3 at 1 kbar pressure are given in Figure 11. The synthetic carbonatite magma represented by eutectic E_1 dissolves about 20 weight percent La(OH)_2 at the ternary eutectic E at 610°C . With increasing $\text{CO}_2/\text{H}_2\text{O}$ in the liquid, represented by the field boundary along E – a , the solubility of La(OH)_2 rises to 40% at the 700°C piercing point.

In the second set of experiments, JONES AND WYLLIE (1983) and WYLLIE AND JONES (1985) made synthetic mixtures approximating the composition of the Mountain Pass ore body as illustrated in Figure 12. The shaded area represents the chemistry of the ore excluding the rare earth elements. Ca(OH)_2 was added to generate the low-temperature synthetic magma (base of the triangle in Figure 12), and the mixture E is estimated to be close in composition to the quaternary eutectic. The phase fields

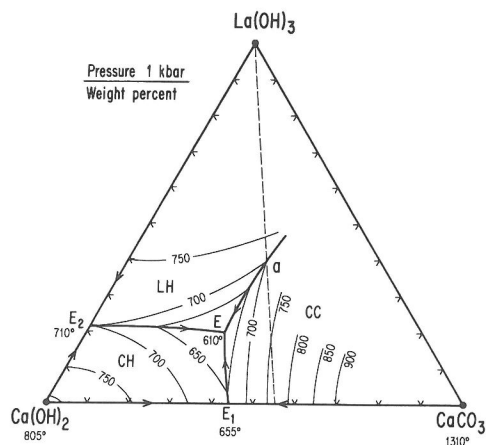


FIG. 11. Preliminary interpretation of ternary liquidus relations in the join CaCO_3 – Ca(OH)_2 – La(OH)_3 at 1 kbar pressure (JONES AND WYLLIE, 1986). Abbreviations: CH = Ca(OH)_2 , LH = La(OH)_3 , CC = CaCO_3 .

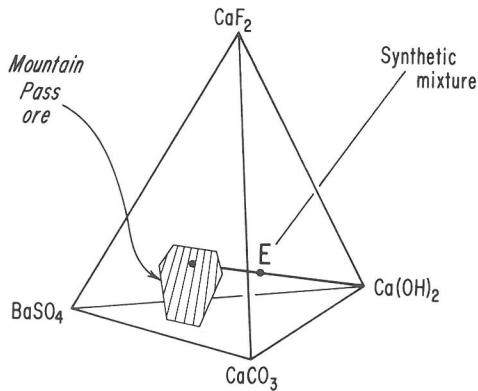


FIG. 12. The mixture E contains 39 weight percent CaCO_3 , 17 weight percent CaF_2 , and 13 weight percent BaSO_4 , representing the Mountain Pass carbonatite ore without rare earth elements, together with 31 weight percent Ca(OH)_2 (JONES and WYLLIE, 1983; WYLLIE and JONES, 1985).

intersected by the composition join E– La(OH)_3 at 1 kbar were determined. The liquidus has a minimum piercing point at 625°C , with 18 weight percent dissolved La(OH)_3 . Phase fields including La-bearing minerals extend from this piercing point. The solidus is at 543°C . Bastnaesite is stable to temperatures of 580°C at this pressure, well above the solidus temperature in Figure 12. Although bastnaesite was not encountered in this composition join, the results suggest that bastnaesite could crystallize along with calcite and barite from a melt of similar composition with suitable proportions of CO_2 , H_2O and F.

Given these experimental results, one might expect that rare earth carbonatites would be more abundant. Probably the biggest factor in precluding the concentration of REE in residual carbonatites is their efficient extraction from the magma by higher-temperature REE-bearing minerals such as perovskite, monazite, and apatite. Therefore, if a parent alkali magma is low in phosphorus and titanium, the potential for differentiation to rare-earth-enriched carbonatite might be enhanced. The occurrence of apatite-rich upper-mantle xenoliths in some locations (WASS *et al.*, 1980) suggests that the heterogeneity of the metasomatized upper-mantle sources might influence the degree of phosphorus-depletion and REE-enrichment in parental magmas derived from HAGGERTY's (1987) mantle metasome layers at level (4) in Figure 6.

SUMMARY OF MAGMATIC AND METASOMATIC EVENTS

(1) The source of volatile components for the genesis of kimberlites and carbonatites is a mantle

reservoir, deeper than the lithosphere and asthenosphere.

(2) The reservoir may include carbon derived from calcite in subducted oceanic basalt, or from limestones (recent subduction only).

(3) Kimberlites may be generated by upward percolation of volatile components, but nephelinites and associated carbonatites require upward movement of solid mantle materials, as a plume or in some other convective mode, followed by lithosphere thinning, and surface rifting.

(4) The asthenosphere–lithosphere boundary layer (near 200 km depth beneath cratons), where the rheology changes from deformable to rigid, is a collecting site for kimberlite magma that is trapped in small dikes or chambers. Temperatures remain too high for solidification of the magma by normal crystallization. Slow reaction of the ilmenite–derived magma with host harzburgite under these conditions, however, is conducive to the growth of large phenocrysts, perhaps corresponding to some of the discrete nodules of kimberlites.

(5) Magmas migrating 5–15 km through the boundary layer approach the solidus, with evolution of a vapor phase. Under suitable stress conditions, the vapor promotes crack propagation, and the kimberlite enters the lithosphere as a dike. Abortion by thermal death and solidification is the fate of most dikes, but sufficiently large reservoirs can yield successive magma pulses through dikes reaching or puncturing the upper crust.

(6) A mantle plume transporting volatile components results in thinning of the lithosphere above it, and accumulation of magma in the asthenosphere–lithosphere boundary layer. Smaller amounts of magma transported by lateral flow in the asthenosphere percolate upward until they lodge in the boundary layer.

(7) Thinning of the lithosphere above the plume, equivalent to upward extension of the deformable asthenosphere, results in the accumulated melt to rise with the isotherms, without crossing the solidus boundary. Intermittent, local excursions of magma to the overlying solidus may be accompanied by vapor release, crack propagation, and magma escape into the developing rift system.

(8) For magma-mantle bodies following a range of depth-temperature trajectories, the ledge on the solidus for peridotite– CO_2 – H_2O is a phase equilibrium barrier to further uprise located at a depth near 75 km. Magmas reaching this barrier evolve vapor and crystallize. The compositions of the vapors evolved, and the crystallization paths of the magmas, vary sensitively according to the position on the solidus boundary reached by the depth-tem-

perature trajectory. Release of vapor promotes crack propagation and eruption of magmas into the rift zone.

(9) Magma-mantle bodies following a trajectory at somewhat higher temperatures miss the phase equilibrium barrier, and these may generate basaltic magmas as they approach the volatile-free peridotite solidus.

(10) Kimberlites and other magmas freed from their mantle host at greater depth are not affected by the phase equilibrium barrier (which is relevant only for melts in equilibrium with peridotite).

(11) Metasomatism may result from reaction of mantle with melts or with vapors, entering or passing through a region. Metasomatic vapors (or solutions) in the subcratonic lithosphere are given off by magmas.

(12) There are two levels in the lithosphere where metasomatic effects should be most prominent. The depleted, refractory base of the lithosphere, 150–200 km deep, has been intermittently invaded by small bodies and dikes of kimberlite, through billions of years, and most of these aborted and gave off vapors. Whenever the craton was rifted, lithospheric thinning was accompanied by the release of abundant vapors at depth near 75 km. Those released at greater depths were enriched in H_2O , and those at shallow depths were enriched in CO_2 .

(13) Parent magmas for melilitites and nephelinites are derived from depths near the phase equilibrium ledge, where extensive metasomatism has occurred.

(14) Nephelinites differentiate to carbonatites, and carbonatites themselves differentiate. Rarely, carbonatites differentiate to rocks with extraordinary enrichment in rare earth elements.

(15) The occurrence of rare earth titanates in mantle metasomatites from 70–100 km depth could be an important factor in the availability of rare earth elements in nephelinites and carbonatites derived from this level.

(16) The extreme concentration of rare earth elements in some differentiated carbonatites is probably due to the paucity of phosphorus in parental melts, and this also could be related to metasomatic events at the 75 km level, events involving apatite.

(17) Kimberlites, and rift valley magmas, are melts with histories involving more than one mantle source material. Both start as melts formed in fertile asthenosphere lherzolite, enriched by migration of vapors from deeper levels. Both spend time residing in contact with the depleted keel of the lithosphere, comprising harzburgite and lherzolite. Kimberlites are erupted from this level. Nephelinites and related magmas are developed by progressive evolution of

kimberlite-like magma as it rises through the lithosphere, increasing in melt fraction until it reaches the 75 km level. The magma may here be enriched by solution of metasomatites formed during a previous occurrence of rifting and magmatic processes.

CONCLUDING REMARKS

The details of what happens where, in the process of transfer of carbon from the mantle to the surface, obviously depend critically on the oxygen fugacity as a function of depth (Figure 2). The changing estimates of mantle oxygen fugacity through the past decade suggest that a complete answer has not yet been achieved. It may become established that the solidus for peridotite-C-H-O depicted in Figure 2 in fact lies at higher temperature, and is not intersected by the normal geotherm. Even if it proves, however, that the deep gases are too reduced to initiate melting at deep level (2), there is petrological evidence that kimberlite melts are erupted from depths of 200 km or so, the lithosphere-asthenosphere boundary level (1) in Figure 2. Therefore, the geotherm and solidus must intersect at 200 km or deeper from time to time and from place to place, either by local oxidation (lowering solidus temperatures) or by local heating (raising the geotherm).

The composition of magmas is controlled not only by the composition of the source material and the degree of melting and fractionation, but by the physical properties of rock-fluid systems. At every stage in the processes outlined in Figure 6, one needs to know the conditions for melt or vapor to flow through, to accumulate in, or to escape from a rock matrix, for rocks that are themselves deforming, as in a mantle plume, or for rocks that are rigid and cooler, as in the lithosphere. These topics are addressed by other papers in the Conference Proceedings, but it was evident from discussions during the Conference that there is as yet no consensus about the rheology of mantle-fluid systems.

Acknowledgments—This research was supported by the Earth Sciences section of the U.S. National Science Foundation, grant EAR84-16583. I thank R. J. Floran of Union Oil Research for his encouragement and the Union Oil Company of California Foundation for a tangible contribution to the program.

REFERENCES

- ANDERSEN T., O'REILLY S. Y. and GRIFFIN W. L. (1984) The trapped fluid phase in upper-mantle xenoliths from Victoria, Australia: Implications for mantle metasomatism. *Contrib. Mineral. Petrol.* **88**, 72–85.
- ARTYUSHKOV E. V. and SOBOLEV S. V. (1984) Physics of the kimberlite magmatism. In *Kimberlites. I: Kim-*

- berlites and Related Rocks*, (ed. J. KORNPROBST), pp. 309–322. Elsevier.
- BOYD F. R. and GURNEY J. J. (1982) Low-calcium garnets: keys to craton structure and diamond crystallization. *Carnegie Inst. Wash. Yearb.* **81**, 261–267.
- BOYD F. R. and GURNEY J. J. (1986) Diamonds and the African lithosphere. *Science* **232**, 472–477.
- BREY G., BRICE W. R., ELLIS D. J., GREEN D. H., HARRIS K. L. and RYABCHIKOV I. D. (1983) Pyroxene–carbonate reactions in the upper mantle. *Earth Planet. Sci. Lett.* **62**, 63–74.
- DEINES P. (1980) The carbon isotopic composition of diamonds: relationship to diamond shape, color, occurrence and vapor compositions. *Geochim. Cosmochim. Acta* **44**, 943–961.
- EGGLER D. H. (1976) Does CO₂ cause partial melting in the low-velocity layer of the mantle? *Geology* **4**, 69–72.
- EGGLER D. H. (1978a) Stability of dolomite in a hydrous mantle, with implications for the mantle solidus. *Geology* **6**, 397–400.
- EGGLER D. H. (1978b) The effect of CO₂ upon partial melting of peridotite in the system Na₂O–CaO–Al₂O₃–MgO–SiO₂–CO₂ to 35 kb, with an analysis of melting in a peridotite–H₂O–CO₂ system. *Amer. J. Sci.* **278**, 305–343.
- EGGLER D. H. and BAKER D. R. (1982) Reduced volatiles in the system C–O–H: implications to mantle melting, fluid formation, and diamond genesis. In *High Pressure Research in Geophysics, Advances in Earth and Planetary Sciences 12*, (eds. S. AKIMOTO and M. H. MANGHNANI), pp. 237–250. Reidel Publishing Co.
- ELLIS D. and WYLLIE P. J. (1979) Carbonation, hydration, and melting relations in the system MgO–H₂O–CO₂ at pressures up to 100 kilobars. *Amer. Mineral.* **64**, 32–40.
- ELLIS D. and WYLLIE P. J. (1980) Phase relations and their petrological implications in the system MgO–SiO₂–CO₂–H₂O at pressures up to 100 kbar. *Amer. Mineral.* **65**, 540–556.
- GLIKO A. O., GRACHEV A. F. and MAGNITSKY V. A. (1985) Thermal model for lithospheric thinning and associated uplift in the neotectonic phase of intraplate orogenic activity and continental rifts. *J. Geodynam. Res.* **3**, 137–153.
- HAGGERTY S. E. (1986) Diamond genesis in a multiply-constrained model. *Nature* **320**, 34–38.
- HAGGERTY S. E. (1987) Source regions for oxides, sulfides and metals in the upper mantle: clues to the stability of diamonds, and the genesis of kimberlites, lamproites and carbonatites. *Proc. Int. Kimb. Conf. 4th, Perth, Australia, 1986*, (In press).
- HAGGERTY S. E., ERLANK A. J. and GREY I. E. (1986) Metasomatic mineral titanate complexing in the upper mantle. *Nature* **319**, 761–763.
- HEINRICH E. W. (1966) *The Geology of Carbonatites*, 555 pp. Rand McNally.
- HOLLOWAY J. R. and JAKOBSSON S. (1986) Volatile solubilities in magmas: transport of volatiles from mantles to planet surfaces. *J. Geophys. Res.* **91**, #B4, D505–508.
- HUANG W. –L., WYLLIE P. J. and NEHRU C. E. (1980) Subsolvus and liquidus phase relationships in the system CaO–SiO₂–CO₂ to 30 kbar with geological applications. *Amer. Mineral.* **65**, 285–301.
- HUANG W. –L. and WYLLIE P. J. (1984) Carbonation reactions for mantle lherzolite and harzburgite. *Proc. 27th Int. Geol. Cong., Moscow 9*, 455–473, VNU Science Press.
- JONES A. P. and WYLLIE P. J. (1983) Low-temperature glass quenched from a synthetic rare-earth carbonatite: implications for the origin of the Mountain Pass deposit, California. *Econ. Geol.* **78**, 1721–1723.
- JONES A. P. and WYLLIE P. J. (1986) Solubility of rare earth elements in carbonatite magmas, indicated by the liquidus surface in CaCO₃–Ca(OH)₂–La(OH)₃ at 1 kbar pressure. *Appl. Geochem.* **1**, 95–102.
- LE BAS M. J. (1977) *Carbonatite–Nephelinite Volcanism*. Wiley and Sons. 347 pp.
- MEYER H. O. A. (1985) Genesis of diamond: a mantle saga. *Amer. Mineral.* **70**, 344–355.
- MYSEN B. O. and BOETTCHER A. L. (1975) Melting of a hydrous mantle. *J. Petrol.* **16**, 520–593.
- OLAFSSON M. and EGGLER D. H. (1983) Phase relations of amphibole, amphibole–carbonate, and phlogopite–carbonate peridotite: petrologic constraints on the asthenosphere. *Earth Planet. Sci. Lett.* **64**, 305–315.
- OTTO J. (1984) Melting relations in some carbonate–silicate systems: sources and products of CO₂-rich liquids. Ph.D. Dissertation, Univ. of Chicago.
- OTTO J. W. and WYLLIE P. J. (1983) Phase relations on the join calcite–nepheline–albite at 25 kb: Subducted basalt limestone as magmatic source (abstr.). *EOS* **64**, 897.
- PECORA W. T. (1956) Carbonatites: a review. *Bull. Geol. Soc. Amer.* **67**, 1537–1556.
- RINGWOOD A. E. (1975) *Composition and Petrology of the Earth's Mantle*, McGraw-Hill.
- RYABCHIKOV I. D., GREEN D. H., WALL W. J. and BREY G. P. (1981) The oxidation state of carbon in the reduced-velocity zone. *Geochem. Int.* **1981**, 148–158.
- SOBOLEV N. V. (1977) *Deep-Seated Inclusions in Kimberlite and the Problem of the Composition of the Upper Mantle*. Amer. Geophys. Union. 279 pp.
- SPERA F. J. (1984) Carbon dioxide in petrogenesis III: role of volatiles in the ascent of alkaline magma with special reference to xenolith-bearing mafic lavas. *Contrib. Mineral. Petrol.* **88**, 217–232.
- TAKAHASHI E. and SCARFE C. M. (1985) Melting of peridotite to 14 GPa and the genesis of komatiite. *Nature* **315**, 566–568.
- WASS S. Y., HENDERSON P. and ELLIOTT C. (1980) Chemical heterogeneity and metasomatism in the upper mantle—evidence from rare earth and other elements in apatite-rich xenoliths in basaltic rocks from eastern Australia. *Philos. Trans. Roy. Soc. London A297*, 333–346.
- WENDLANDT R. F. (1984) An experimental and theoretical analysis of partial melting in the system KAlSiO₄–CaO–MgO–SiO₂–CO₂ and applications to the genesis of potassic magmas, carbonatites and kimberlites. In *Kimberlites. I: Kimberlites and Related Rocks*, (ed. J. KORNPROBST), pp. 359–369. Elsevier.
- WENDLANDT R. F. and EGGLER D. H. (1980) The origins of potassic magmas: II. Stability of phlogopite in natural spinel lherzolite and in the system KAlSiO₄–MgO–SiO₂–H₂O–CO₂ at high pressures and high temperatures. *Amer. J. Sci.* **280**, 421–458.
- WENDLANDT R. F. and MORGAN P. (1982) Lithospheric thinning associated with rifting in East Africa. *Nature* **298**, 734–736.
- WENDLANDT R. F. and MYSEN B. O. (1980) Melting phase relations of natural peridotite + CO₂ as a function of

- degree of partial melting at 15 and 30 kbar. *Amer. Mineral.* **65**, 37–44.
- WOERMANN E. and ROSENHAUER M. (1985) Fluid phases and the redox state of the Earth's mantle: extrapolations based on experimental, phase-theoretical and petrological data. *Fortschr. Mineral.* **63**, 263–349.
- WYLLIE P. J. (1977) Mantle fluid compositions buffered by carbonates in peridotite–CO₂–H₂O. *J. Geol.* **85**, 187–207.
- WYLLIE P. J. (1978) Mantle fluid compositions buffered in peridotite–CO₂–H₂O by carbonates, amphibole, and phlogopite. *J. Geol.* **86**, 687–713.
- WYLLIE P. J. (1979) Magmas and volatile components. *Amer. Mineral.* **64**, 469–500.
- WYLLIE P. J. (1980) The origin of kimberlites. *J. Geophys. Res.* **85**, 6902–6910.
- WYLLIE P. J. (1987) Metasomatism and fluid generation in mantle xenoliths: experimental. In *Mantle Xenoliths*, (ed. P. H. NIXON), Wiley, (In press).
- WYLLIE P. J. and HUANG W. –L. (1975) Peridotite, kimberlite, and carbonatite explained in the system CaO–MgO–SiO₂–CO₂. *Geology* **3**, 621–624.
- WYLLIE P. J. and JONES A. P. (1985) Experimental data bearing on the origin of carbonatites, with particular reference to the Mountain Pass rare earth deposit. In *Applied Mineralogy*, (eds. W. C. PARK, D. M. HAUSEN and R. D. HAGNI), 935–949. Amer. Inst. Mining, Metallurgical, and Petroleum Engineers, Inc., New York.
- WYLLIE P. J. and RUTTER M. (1986) Experimental data on the solidus for peridotite–CO₂, with applications to alkaline magmatism and mantle metasomatism (abstr.). *EOS* **67**, 390.
- WYLLIE P. J., HUANG W. –L., OTTO J. and BYRNES A. P. (1983) Carbonation of peridotites and decarbonation of siliceous dolomites represented in the system CaO–MgO–SiO₂–CO₂ to 30 kbar. *Tectonophys.* **100**, 359–388.

